

**PROBING THE VIBRATIONAL RELAXATION OF N₂ AND O₂ BY
USE OF CARS SPECTROSCOPY TO MODEL NTE-TURBULENCE**

A Senior Scholars Thesis

by

JACOB DEAN

Submitted to the Office of Undergraduate Research
Texas A&M University
in partial fulfillment of the requirements for the designation as

UNDERGRADUATE RESEARCH SCHOLAR

April 2009

Major: Chemistry

**PROBING THE VIBRATIONAL RELAXATION OF N₂ AND O₂ BY
USE OF CARS SPECTROSCOPY TO MODEL NTE-TURBULENCE**

A Senior Scholars Thesis

by

JACOB DEAN

Submitted to the Office of Undergraduate Research
Texas A&M University
in partial fulfillment of the requirements for the designation as

UNDERGRADUATE RESEARCH SCHOLAR

Approved by:

Research Advisor:
Associate Dean for Undergraduate Research:

Simon North
Robert C. Webb

April 2009

Major: Chemistry

ABSTRACT

Probing the Vibrational Relaxation of N₂ and O₂ by Use of CARS Spectroscopy to Model NTE-Turbulence. (April 2009)

Jacob Dean
Department of Chemistry
Texas A&M University

Research Advisor: Dr. Simon North
Department of Chemistry

The thermochemical dynamics associated with hypersonic flight and turbulent flow is vital to understanding the effects that hypersonic turbulence has on objects or vehicles traveling at speeds above Mach 5 (~ 1708 m/s). Non-thermochemical equilibrium (NTE) exists downstream of strong shock fronts and encountered in the shear layers from hypersonic flight, and coupled with turbulence, it has significant effects on flow dynamics. NTE, characterized by high vibrational temperatures of N₂ and O₂, was observed, and the relaxation processes were measured to obtain time-resolved results. By inducing cold-flow NTE via RF-plasma, species in the flow were probed to determine specific vibrational temperatures at particular distances and times following initial NTE-preparation. The detection technique used in the experiment was coherent anti-Stokes Raman spectroscopy (CARS) and variations of this laser-based technique were optimized to maximize accuracy and signal-to-noise in the vibrational relaxation measurements. It was found that the boxCARS variant was most successful in probing the $v=1 \rightarrow v=0$ vibrational transition associated with the measurement. Also a dual

pump-beam CARS setup enabled the probing of both N_2 and O_2 simultaneously; however, in this report only N_2 vibrational relaxation was modeled because the lifetime of vibrationally-excited ($v=1$) O_2 was too short and the O_2 vibrational temperature was too low to model. The CARS spectra were obtained in a subsonic wind tunnel with a flow velocity of approximately 30 m/s and probing distances from 4.4-39.4 cm downstream the plasma. Five averaged vibrational temperature values were determined and they yielded a decay from 1882 ± 46 K (4.4 cm from plasma) to 1010 ± 16 K (39.4 cm from plasma) showing the relative rate of vibrational relaxation of N_2 . The vibrational relaxation was also modeled as a function of time after passing through the plasma, and a kinetic simulation was fit to the results. The spectral decay of the $v=1$ peak relative to $v=0$ ($I_{v=1}/I_{v=0}$) was found and compared to the decay of the vibrational temperature. Data analysis revealed that the results were in agreement with theory and the observed vibrational relaxation of N_2 fit the simulated kinetic model accurately.

ACKNOWLEDGMENTS

The invaluable help and direction of Dr. Simon North, Dr. Rodney Bowersox, Rodrigo Sanchez-Gonzalez, and Andrea Hsu must be acknowledged. As my research advisor, Dr. Simon North has been an incredible asset to my understanding of the chemistry and methodology of the research performed. Also, Rodrigo Sanchez-Gonzalez and Andrea Hsu have been both helpful and patient with my learning throughout this research experience. Their work and knowledge made the project possible and my gratitude goes to them.

Dr. Rodney Bowersox and his group have been key contributors to the NTE research in general, and their engineering accomplishments have been essential components to the project. TJ Fuller must be acknowledged for his work in the construction of the NTE tunnel. The United States Air Force must also be mentioned due to their care and support in the topic being researched. The contributions of each individual's knowledge and experience have facilitated the learning process throughout the research performed, and without their contributions this opportunity would not have been possible.

Lastly, I am grateful for the support and inspiration from my parents, Billy and Joyce Dean, as well as the friendship and constant motivation from my sister, Jenny Dean.

NOMENCLATURE

a.u.	Arbitrary Units
CARS	Coherent Anti-Stokes Raman Spectroscopy
CCRF	Capacitively Coupled Radio-Frequency
CFD	Computational Fluid Dynamics
FWHM	Full Width at Half Maximum [intensity of line]
Hypersonic	Flow Speed More Than 1708 m/s
I	Spectral Intensity (units arbitrary)
k	Boltzmann Constant
λ	Wavelength (nm)
m/s	Meters/Second
$N_{v=i}$	Population of Vibrational Level <i>i</i>
NTE	Non-Thermochemical Equilibrium
ω_i	Frequency of Photon <i>i</i>
P	Pressure
S/N	Signal/Noise Ratio
Subsonic	Flow Speed Less Than 341.5 m/s
Supersonic	Flow Speed Between 409.8 m/s – 1708 m/s
T_r	Rotational Temperature (K)
T_v	Vibrational Temperature (K)

TABLE OF CONTENTS

	Page
ABSTRACT	iii
ACKNOWLEDGMENTS.....	v
NOMENCLATURE.....	vi
TABLE OF CONTENTS	vii
LIST OF FIGURES.....	viii
LIST OF TABLES	x
 CHAPTER	
I INTRODUCTION.....	1
Non-thermochemical equilibrium	1
Probing N ₂ and O ₂ vibrational relaxation	2
Coherent anti-Stokes Raman spectroscopy	4
II METHODS.....	8
Phase-matching schemes for CARS.....	8
Experimental setup	13
Data processing	18
III RESULTS.....	22
Pre-NTE measurements.....	22
Measurement of vibrational relaxation in NTE-turbulent flow	29
IV SUMMARY AND CONCLUSIONS.....	41
REFERENCES.....	44
CONTACT INFORMATION	45

LIST OF FIGURES

FIGURE	Page
1 Energy level scheme of CARS process.....	5
2 Dual-pump CARS energy scheme	6
3 Beam paths for (a) collinear variant and (b) boxCARS variant.....	9
4 Broadband dye laser dye curve	10
5 Rhodium atomic lines with dye curve.....	11
6 Broadband laser with labeled components.....	12
7 Beam paths and interaction in dual-pump CARS	13
8 Experimental schematic of (a) single-species CARS and (b) dual-pump CARS used in the experiment.....	15
9 Dual-pump CARS experimental setup for standard measurements.....	16
10 Picture of CARS experiment in progress	17
11 Schematic of NTE wind tunnel with test section	18
12 Theoretical CARS spectra for N ₂ at various vibrational temperatures	19
13 N ₂ experimental emission spectrum and best-fit emission spectrum.....	23
14 Collinear-CARS spectrum of N ₂ at 1 atm and 298 K.....	24
15 Collinear-CARS spectrum of N ₂ in propane flame	25
16 BoxCARS spectrum of N ₂ in ambient air	26
17 (a) Experimental CARS spectrum of N ₂ in propane/air flame with theoretical fit. (b) Chi-square plot of N ₂ flame spectrum compared with calculated spectra at various T _v	27
18 Dual-pump CARS spectrum of N ₂ and O ₂ at 1 atm and ~298 K	29

FIGURE	Page
19 Dual-pump CARS spectrum 4.4 cm downstream	30
20 (a) Schematic of measurement positions. (b) Test section used in the experiment	31
21 (a) N ₂ CARS spectrum 4.4 cm downstream with best-fit theoretical spectrum. (b) Chi-square plot of N ₂ spectrum compared with calculated spectra at various T _v	33
22 N ₂ CARS spectrum 7.9 cm downstream with best-fit theoretical spectrum	34
23 N ₂ CARS spectrum 20.0 cm downstream with best-fit theoretical spectrum	35
24 N ₂ CARS spectrum 26.5 cm downstream with best-fit theoretical spectrum	36
25 N ₂ CARS spectrum 39.4 cm downstream with best-fit theoretical spectrum	37
26 N ₂ T _v decay under NTE-turbulence with time (μs) and distance downstream (cm)	38
27 %v=1 spectral-intensity decay with distance along flow axis	39

LIST OF TABLES

TABLE	Page
1 T_v and $I_{v=1}/I_{v=0}$ data observed at distances down the flow-axis, z , when $z_0 =$ distance at plasma	40

CHAPTER I

INTRODUCTION

Non-equilibrium systems occur prominently in nature. Given the state of nature itself, it only seems plausible that most systems whether biological or chemical exist in non-equilibrium. Phenomena occurring in real, non-equilibrium systems are continuously transmitting energy to the system's open surroundings and interacting with systems in the near-environment. By this idea, many phenomena existing in non-equilibrium domain can be difficult to study due to the violation of many assumptions in equilibrium thermodynamics and due to the required time resolution. However, fluid flows and gas flows are often non-equilibrium systems that can efficiently be studied by use of laser diagnostics to measure flow parameters and molecular velocities resolved in time. In high-speed air flows reaching supersonic and hypersonic speeds, thermochemistry can display relevant data to characterize the air flow and the states of the species involved.

Non-thermochemical equilibrium

Non-thermochemical equilibrium (NTE) exists in hypersonic-turbulent flows, and theoretical evidence shows that NTE has effects on the turbulence in the high-speed air flow. When an object reaches hypersonic speeds intense shock waves are produced in the flow-front and internal energy modes in air molecules are excited. The excited states

This thesis follows the style of *Journal of Raman Spectroscopy*.

subsequently relax back down to equilibrium upon the dissipation of the shock waves, and the timescale of the vibrational relaxation process is comparable to that of the turbulence timescales in hypersonic flows. This fact provides evidence of the coupling that exists between NTE and turbulence. The effects of NTE-turbulence coupling can be observed by a variety of laser-based techniques to determine velocities and time-resolved excited-state relaxation of the air molecules interacting with the shock induced by hypersonic speeds. Previous calculations have been done to theorize the effects of NTE on hypersonic vehicles;¹⁻² however, few studies have provided the computations necessary to sufficiently reduce the negative effects of turbulence on hypersonic vehicles to maximize the overall efficiency of flight. A model that gives reliable data on NTE-turbulence at hypersonic speeds could provide effective elements for future hypersonic research as well as an understanding of the thermochemistry of air in NTE systems. The experimental calculations used to model the NTE effects are in line with computational fluid dynamics (CFD) simulations to serve as a reference and counterpart. The theoretical model is a compilation of various components that each target an effect displayed by NTE turbulence. One primary component of NTE turbulence that yields information on the energy transmission in the flow is the vibrational relaxation of air molecules in the system.

Probing N₂ and O₂ vibrational relaxation

During hypersonic flight, NTE conditions are manifested thermally at temperatures up to 10000 K; however, for practical measurements this can be very difficult to reproduce

and inherently more complex because the air molecules involved dissociate to form a mixture of flow components altering the composition of the flow. To replicate the induction of NTE in a laboratory facility, a capacitively coupled radio-frequency (CCRF) plasma spanning the cross-section of a wind tunnel excites the air molecules in the flow creating cold-flow NTE. Shortly after passing through the RF-generated plasma the excited molecules readily transfer the excess vibrational energy via quantum pathways such as quenching, molecular translation and rotation to return to their energetic ground state. By studying the rate of vibrational relaxation of air molecules (N_2 and O_2) in the flow, appropriate data analysis and simulations can display the pathways for energy loss, subsequently yielding information on the coupling of NTE and turbulence. The energy transmission between vibrational modes of molecules in the flow can be modeled by measuring the vibrational temperatures along the test section downstream from the plasma.³ The vibrational temperature, energy difference between vibrational states, and populations of vibrational states are all correlated by the Boltzmann distribution given by:

$$\frac{N_{v=es}}{N_{v=0}} = \exp\left(\frac{-\Delta E}{kT_v}\right) \quad (1)$$

where $N_{v=0}$ is the population of ground vibrational level $v=0$, $N_{v=es}$ is the population of a vibrational excited state, ΔE is the difference in energy between the two levels, k is the Boltzmann constant and T_v is the vibrational temperature. The method used to probe the relative vibrational modes of N_2 and O_2 in the flow is known as coherent anti-Stokes

Raman spectroscopy (CARS). Temperature, whether translational, vibrational, or rotational can be experimentally derived from the shape of the CARS spectrum itself.⁴

Coherent anti-Stokes Raman spectroscopy

CARS is a spectroscopy technique based on the Raman effect and coherent Raman scattering. Unlike spontaneous Raman spectroscopy where inelastic Raman scattering must be extracted through the prevalent Rayleigh scattering, the Raman signal is coherent in a single beam giving a signal of 10^6 times more strength.^{5,6} The coherent nature of CARS enables clean probing of gas molecules traveling in a turbulent flow without loss of signal.⁶ The CARS phenomenon involves the coherent interaction of three photons at particular frequencies resonant with specific vibrational modes of the species under study. The result is a three-wave mixing process that begins with two photons at frequencies ω_{P1} and ω_s exciting the molecule to a Raman active vibrational level, and a third photon ω_{P2} that probes the excited state resulting in a signal photon at the anti-Stokes frequency of the species defined as:⁷⁻¹⁰

$$\omega_{as} = \omega_{P1} - \omega_s + \omega_{P2} \quad (2)$$

The energy level diagram of the CARS process is shown in figure 1.⁹

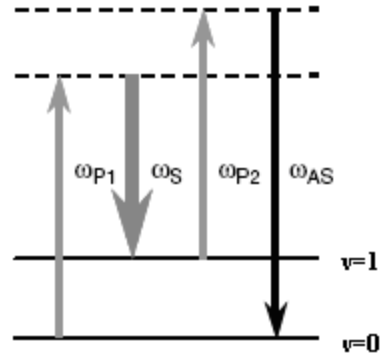


Figure 1. Energy level scheme of CARS process

The ω_p photons in equation 2 and figure 1 represent pump photons and the ω_s photon is at the Stokes frequency. It can be seen from figure 1 that the difference in the frequency of the ω_{p1} beam and the Stokes beam ω_s must be equal to one Raman-active vibrational mode of the molecule under study.^{4,9} Taking advantage of the CARS process, different vibrational states of N_2 and O_2 can be probed to determine the vibrational temperatures of the molecules at positions relative to the RF-plasma. By measuring the decay of the $v=1$ state back down to the ground vibrational state ($v=0$), the relaxation kinetics can be modeled and related to NTE-turbulence effects. The Boltzmann distribution given in equation 1 can then be rewritten to reflect the $v=1 \rightarrow v=0$ vibrational band:

$$\frac{N_{v=1}}{N_{v=0}} = \exp\left(\frac{-\Delta E}{kT_v}\right) \quad (3)$$

The flow velocity in the subsonic NTE facility is approximately 30 m/s (Mach 0.088) and the vibrational relaxation of N_2 and O_2 were measured at these low speeds to model the patterns in kinetics before hypersonic testing.

Simultaneous measurement with dual-pump scheme

One of the prominent advantages of CARS is its specificity toward target molecular species. However, a consequence of its specificity leads to an inherent disadvantage in probing multiple species. Given the frequency limits of the photon interactions shown in equation 2, the multiple beam setup seems to only be applicable to a specific vibrational Raman mode. It has been found though that multiple species can be probed by CARS by employing a dual-pump beam setup where two narrowband laser sources ω_1 and ω_2 (of different wavelengths) and a broadband laser source ω_s can simultaneously probe two species.⁹⁻¹¹ To probe two species, the frequency differences $\omega_1 - \omega_s$ and $\omega_2 - \omega_s$ must equal the corresponding Raman transitions in the system and the results are signals from both species at frequency ω_{as} as shown in equation 4.¹⁰⁻¹¹

$$\omega_{as} = \omega_1 - \omega_s + \omega_2 = \omega_2 - \omega_s + \omega_1 \quad (4)$$

An energy level diagram displaying the dual-pump CARS process for species i and j is shown in figure 2.¹¹

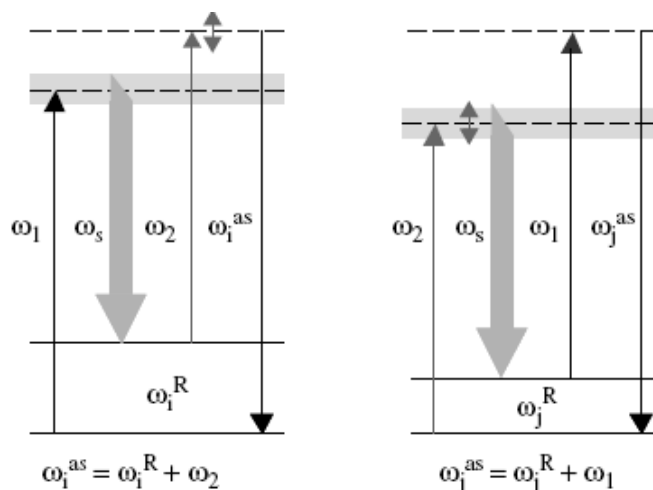


Figure 2. Dual-pump CARS energy scheme¹¹

Figure 2 shows a representation of the process occurring in the simultaneous probing of N_2 and O_2 where species i is N_2 and species j is O_2 . Conventional CARS done on N_2 and O_2 separately can be used as a standard to validate the data obtained by dual-pump CARS; the advantage of simultaneous measurement is the collection of data from both species under exact quantitative conditions.

CHAPTER II

METHODS

Phase-matching schemes for CARS

Various beam configurations have been applied in CARS experiments. Typically, if the phase-matching conditions of the beams are met and the signal corresponds to a Raman mode (defined by equation 2), the CARS phenomenon occurs. The beam configurations tested in the experiment were collinear CARS and boxCARS. The collinear variant of CARS is relatively simple to setup because it only requires the wave vectors (beams) k_1 and k_s to traverse parallel to each other as they enter the lens for CARS interaction as seen in figure 3(a).⁶ The primary issue in using the collinear variant to obtain spectra of vibrationally-excited molecules is the length of the interaction region that defines the probing length. The interaction region is the point in space where the three photons meet and yield the anti-Stokes photon ω_{as} . As seen from figure 3(a), the paths of the beams between the lenses are practically overlapped; this is problematic in the experiment because the test section is a fixed width and if the interaction region is very large, much of the air outside of the test section is probed giving an over-representation of ground state N_2 and O_2 relative to the vibrationally-excited molecules existing inside the test section. To alleviate the problem, the boxCARS beam configuration was used to minimize the length of the interaction region and ensure that the vibrational band was probed precisely. As shown in figure 3(b),⁶ the planar boxCARS geometry requires two pump beams and a Stokes beam; one pump beam, k_p , traverses overlapped to the Stokes

beam k_s , while the other enters the lens parallel to them. The entry points of the beams into the lens causes the beams to cross in-plane at the focal point and enter into another lens of equal focal length to yield four collimated beams including the k_{as} beam carried out by the single k_p beam.

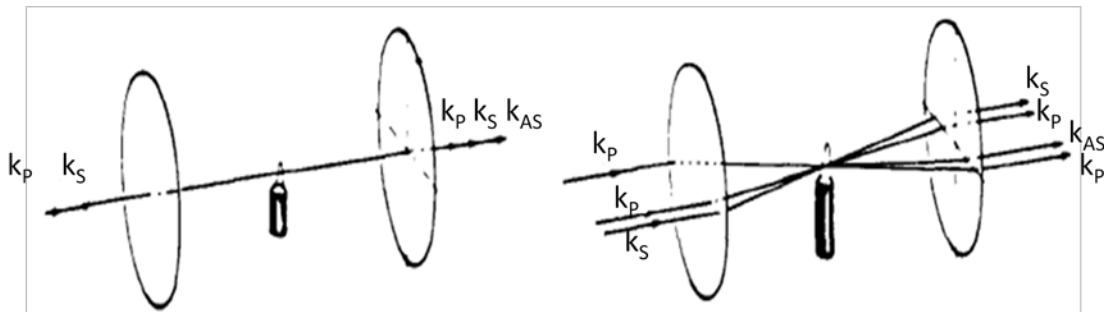


Figure 3. Beam paths for (a) collinear variant and (b) boxCARS variant⁶

The in-plane crossing of the boxCARS variant minimizes the interaction region allowing for an accurate anti-Stokes signal to emerge. Given that the crossing angle, α , was less than 35° , the interaction length, l , can be defined by the following equation:⁷

$$l = d_1(2 \sin \alpha)^{-1} \quad (5)$$

where d_1 is the pump beam diameter. By equation 5 it can be seen that as the crossing angle decreases or the beam diameter increases, the interaction length increases and limits the precision on vibrational measurements. The advantages of boxCARS make it the primary method for obtaining spatially-resolved vibrational CARS spectra.⁶⁻⁷

Beam sources

For CARS on separate measurements of N_2 or O_2 , the pump beams, k_p , were both at $\lambda=532$ nm from the second harmonic of a Quanta-Ray Nd:YAG laser and the Stokes

beam, k_s , was from a broadband dye laser lasing at a peak wavelength $\lambda=606$ nm and pumped by the split Nd:YAG beam. The broadband dye laser must have its peak wavelength at the ω_s wavelength to maximize the intensity of the CARS signal and meet the phase-matching conditions. The dye used as the lasing medium in the broadband source was a mixture of rhodamine 610 (R610) and rhodamine 640 (R640) dye in methanol optimized to the ω_s wavelength; the dye curve of the R610/R640 mixture used in the broadband laser is shown in figure 4.

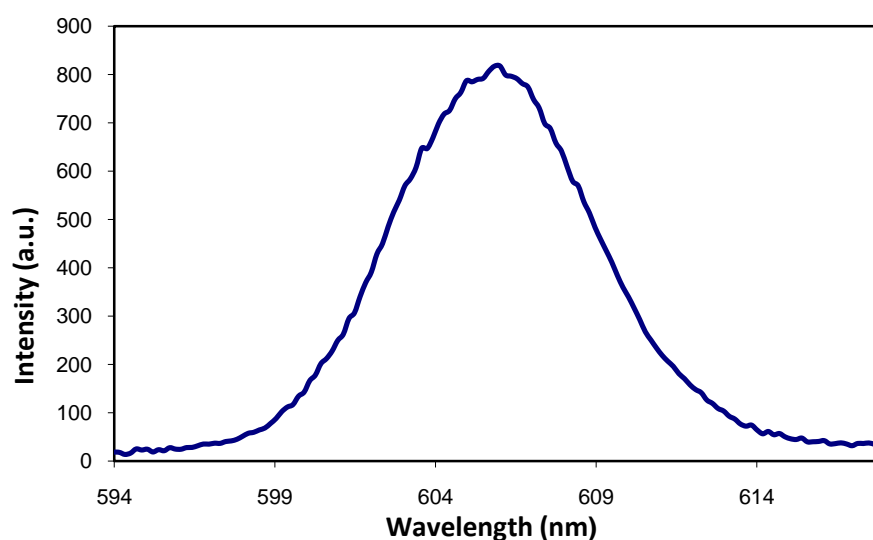


Figure 4. Broadband dye laser dye curve

The dye curve shown in figure 4 was taken by sending the light from the broadband laser directly into the spectrometer. Before the spectrum could be collected the spectrometer had to first be calibrated in terms of wavelength by sending the light from a rhodium hollow-cathode lamp into the spectrometer since the rhodium atomic lines are in the

wavelength region of interest (around 606 nm). The atomic lines of the rhodium hollow-cathode lamp with the dye curve are plotted in figure 5.

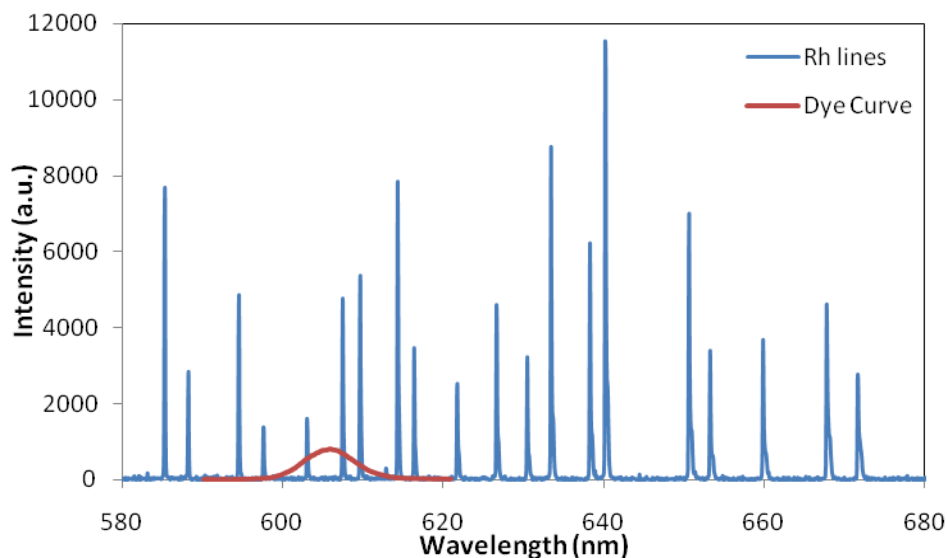


Figure 5. Rhodium atomic lines with dye curve

The broadband laser was built from the parts of a dye laser that was no longer in operation. The placement of the dye cells, prisms, and lenses were all optimized to maximize the output laser energy and the parts were subsequently bolted to a breadboard. The oscillator cavity was composed of a broadband mirror and a quartz plate output-coupler (reflectivity $\sim 10\%$); the oscillator was side-pumped and the amplifier was end-pumped. A picture of the broadband laser that was constructed with labeled components is shown in figure 6.

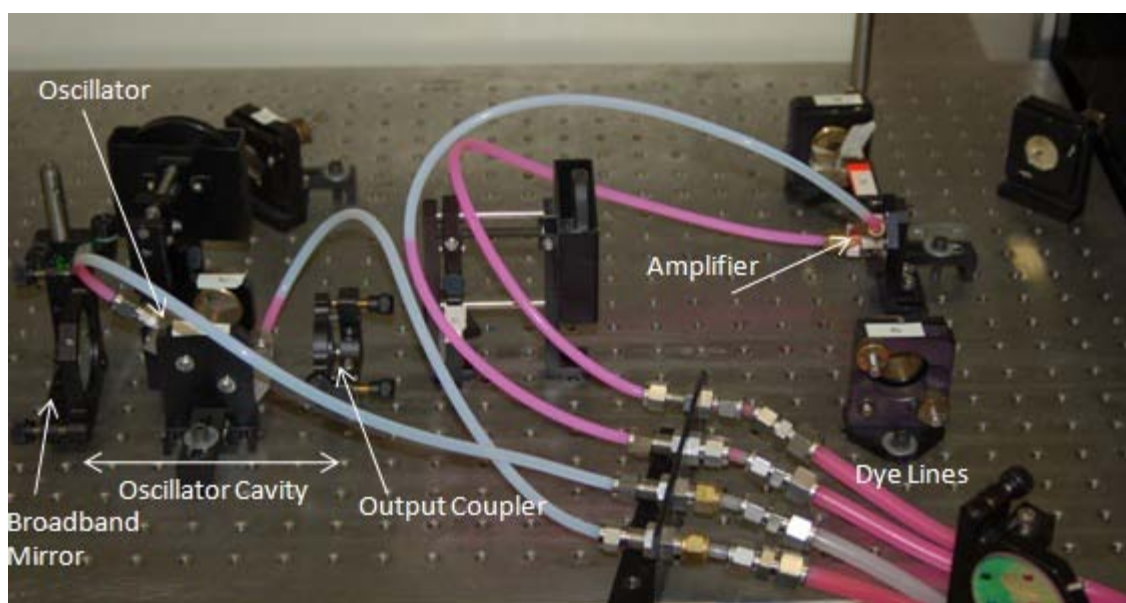


Figure 6. Broadband laser with labeled components

For the simultaneous measurement of N_2 and O_2 via dual-pump CARS, the boxCARS beam configuration was used, but the pump beam parallel to the overlapping pump and Stokes beams was at a wavelength of 555 nm instead of 532 nm. A diagram of the entry and exit points of the dual-pump CARS beams are shown in figure 7.

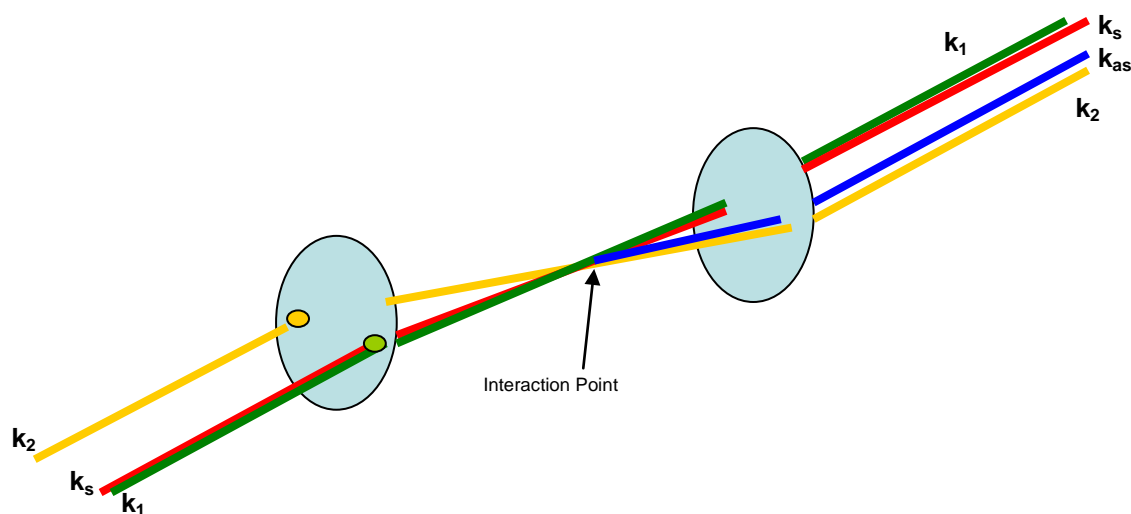


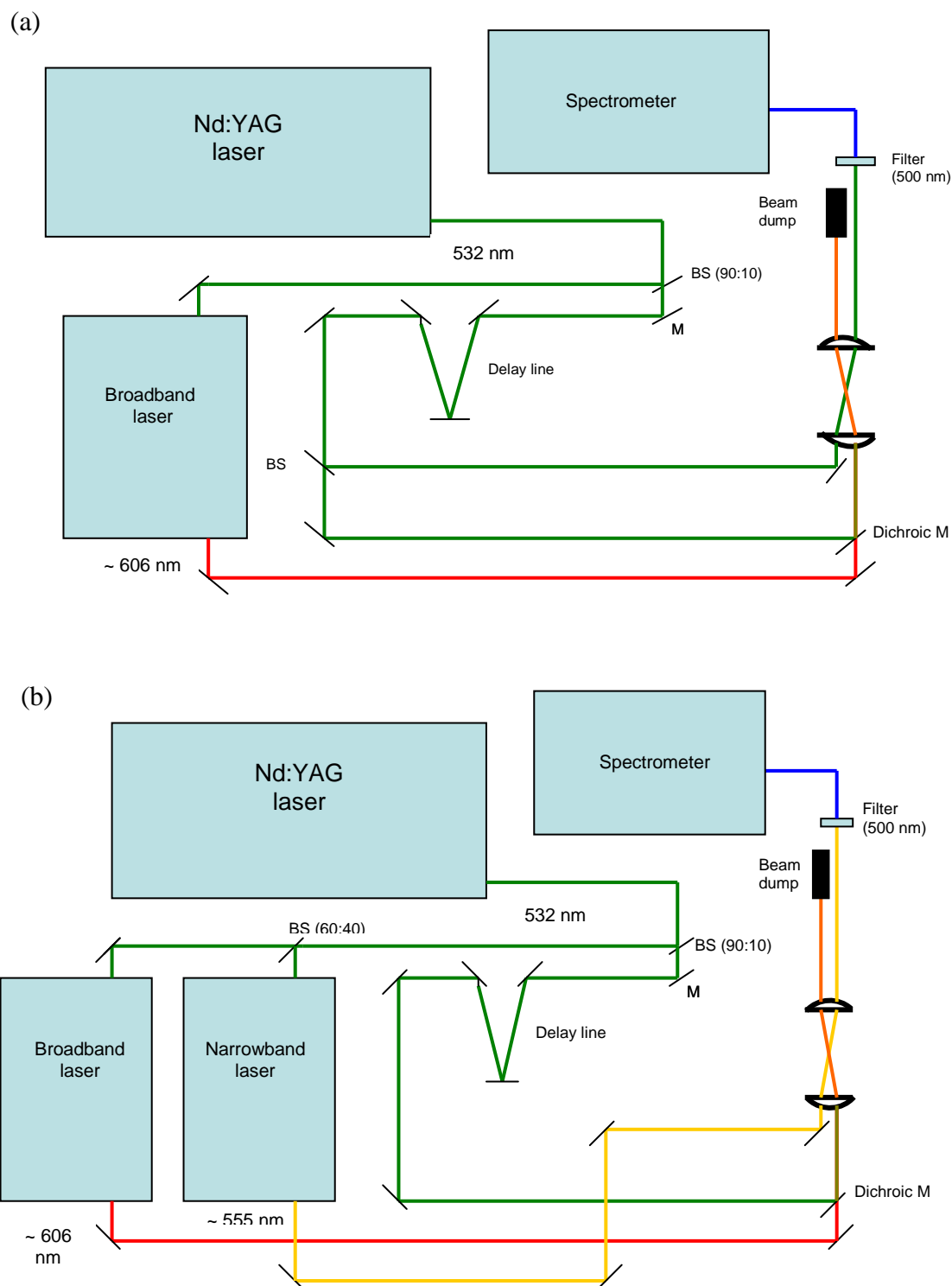
Figure 7. Beam paths and interaction in dual-pump CARS

From equation 4, the source of the ω_2 photons at 555 nm was a narrowband Quanta-Ray PDL-1 dye laser using fluorescein 550 dye in NaOH-methanol solution as the lasing medium.

Experimental setup

The experimental setup for CARS was the most significant factor in obtaining data on the vibrational temperatures and relaxation of N_2 and O_2 . The pathways for the beams and the placement of the optics were vital to the precision of the experiment. In single CARS and dual-pump CARS, a vertically-polarized Nd:YAG laser pulsing at 10 Hz was the starting point of the beam path, and the beam was split by a quartz plate (90:10) to pump the dye laser(s) (90% of beam power) and the rest (10% of beam power) was sent along a path to serve as the pump beam shown in the planar boxCARS configuration in figure 3. In the dual-pump scheme, the beam is split again (60:40) at the narrowband dye

laser to send the remaining 532 nm light into the broadband dye laser. A delay line created by a series of 45° and 0° incidence mirrors had to be introduced into the scheme to account for the different pathways of the various beams. If the beams are not temporally overlapped, no CARS signal is produced (or a very weak signal); this issue was addressed by observing the laser pulses in time with a photodiode and oscilloscope. The length of the delay line was optimized so that the laser pulses overlapped directly both spatially and temporally to ensure maximum CARS interaction. The output of the dye laser(s) were directed by broadband mirrors to end in the appropriate positions at the lens where all of the beams are crossed. To align the 532 nm pump beam and broadband beam collinearly, a dichroic mirror was used for the 606 nm broadband light to pass through to meet collinearly with the pump beam (Nd:YAG light). The schematics of the experimental setup for both single-species CARS and dual-pump CARS are shown in figure 8 (a) and (b) respectively.



After the CARS interaction occurred, the collected signal at 470-490 nm was carried out by the single pump beam and the light was passed through a cutoff filter (filter > 500 nm) to eliminate the pump light. The remaining signal was sent into a 10 cm focal length lens to focus the signal into the entrance slit of the spectrometer. A picture of the dual-pump CARS setup is shown in figure 9. Typically, the experiment was run using 150-200 mJ laser energy from the Nd:YAG laser source and the dye lasers both operate at approximately 5% efficiency (5 mJ dye laser/100 mJ pump laser).

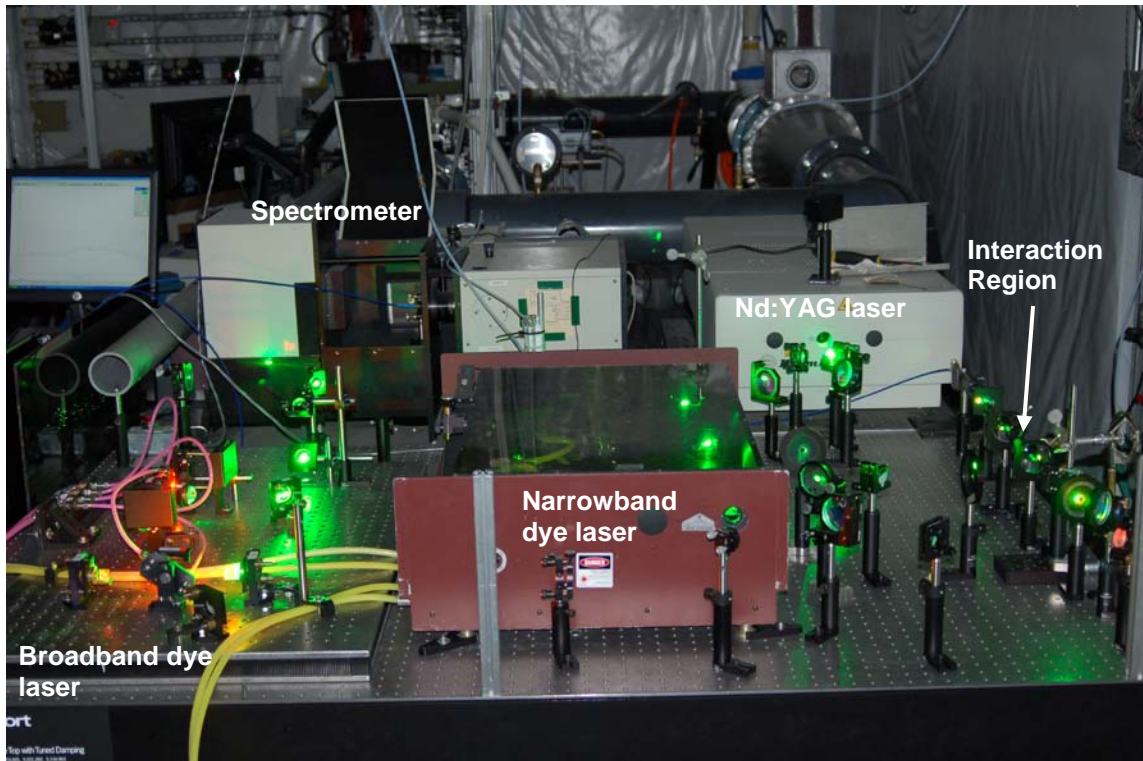


Figure 9. Dual-pump CARS experimental setup for standard measurements

The placement of the optics was on a single table for obtaining CARS spectra in air at 1 atm or in a flame at 1 atm. However for the spectra obtained from the NTE tunnel to

measure the vibrational decay, the optics following the dye laser(s) and the 532 nm pump beams had to be placed near the test section so that the beam crossing-point could be focused in the center of the test section of the NTE tunnel. To run CARS in the NTE tunnel, the beams had to be directed through a PVC pipe (to minimize light scattering) and re-collimated at the other end. Once collimated, the beams were directed into the lens which was placed approximately 1 inch from the test section. The incoming beams directed into the test section are shown in figure 10; the picture was taken while the dual-pump CARS experiment was in progress.

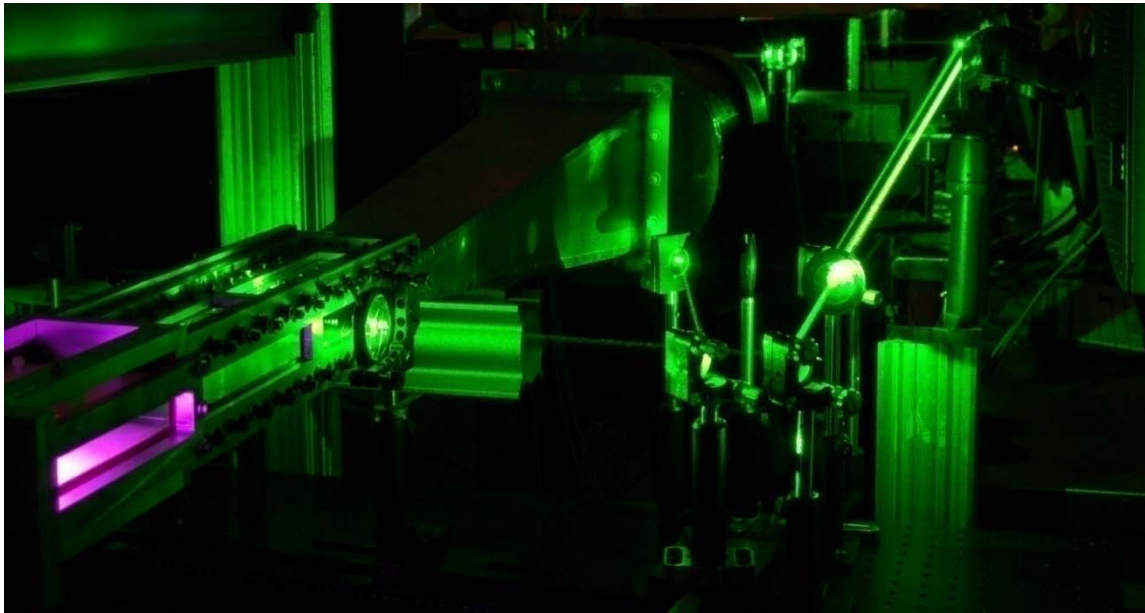


Figure 10. Picture of CARS experiment in progress

As seen in figure 10, the glow coming from the test section is the lit plasma and the three beams are directed into the test section where the CARS interaction took place. The spectrometer was placed behind the filter on the other side of the test section to obtain

the CARS signal and the light was focused into the spectrometer slit. Displayed in figure 11 is a schematic of the NTE subsonic-tunnel and the relative locations of the RF-plasma and test section where the measurements were made.

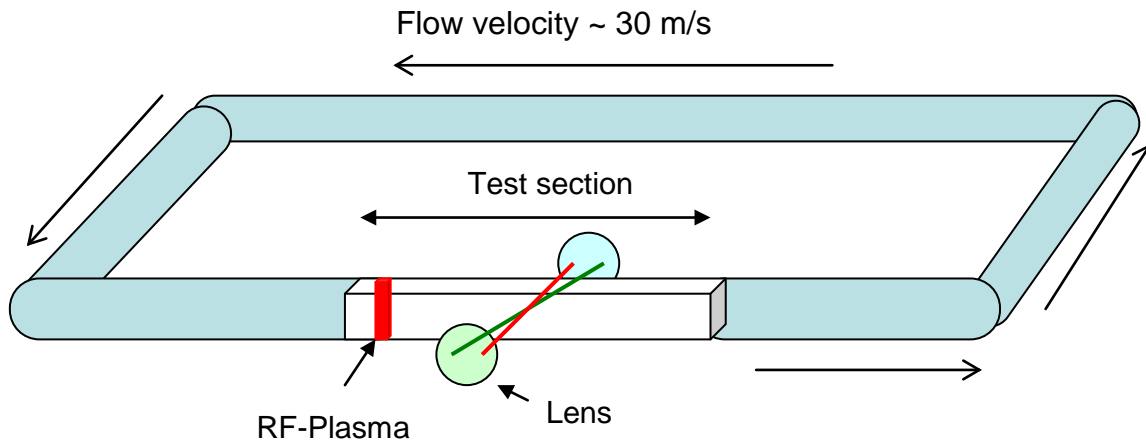


Figure 11. Schematic of NTE wind tunnel with test section

The speed of the flow in the NTE facility was approximately 30 m/s. CARS was performed at subsonic speeds in the experiment to obtain a low-speed model in preparation for measurements in hypersonic air flow.

Data processing

The CARS spectra were obtained by an Andor ICCD (intensified charge-coupled device) camera and the corresponding Andor SOLIS software was used to display the spectra.

To calibrate the spectrometer for accurate wavelength measurements the light from a hollow-cathode lamp was used as a reference as shown in figure 5, and the corresponding spectral lines were matched in the Andor software. After obtaining the

CARS spectra, they were imported into Microsoft Excel for further evaluation. To find the vibrational temperature of N_2 or O_2 after collecting a spectrum, the CARSFIT code¹² developed by Sandia labs was used to calculate a theoretical spectrum based on vibrational and rotational temperatures of the measured species. Parameters adjusted in the CARSFIT code to produce accurate theoretical spectra included: pressure, mole fraction, beam line-width, vibrational temperature T_v , and rotational temperature T_r . In order to fit the theoretical spectrum to the experimental spectrum, the $v=1$ peak had to be distinguishable in the experimental spectrum so that the scaling could be accomplished precisely. Several theoretical spectra were generated to accurately fit a single experimental spectrum. A series of generated theoretical CARS spectra is shown in figure 12 for N_2 ; the vibrational temperatures input into the CARSFIT code for each individual curve were 800 K, 1000 K, 1400 K, 1800 K, and 2400 K.

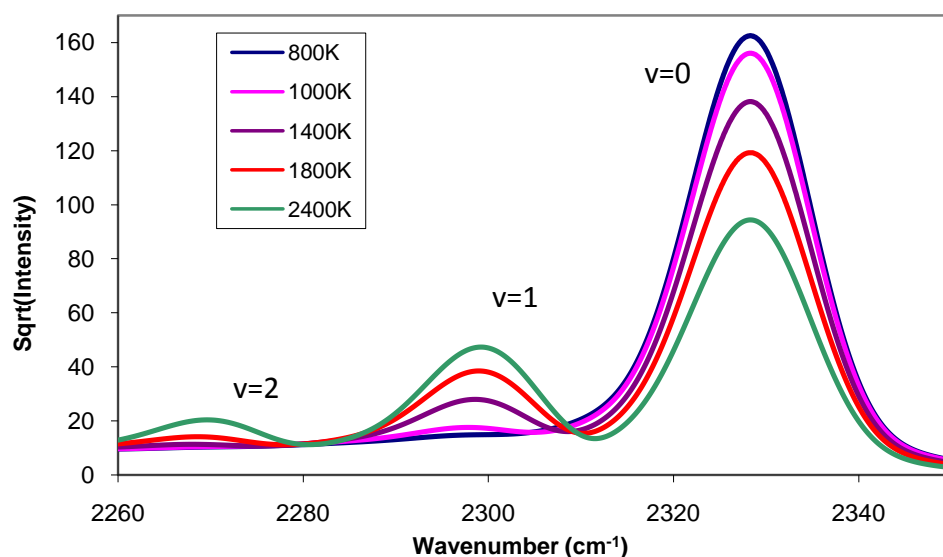


Figure 12. Theoretical CARS spectra for N_2 at various vibrational temperatures

For the calculated N₂ spectra shown in figure 12 the rotational temperature was held constant at 340 K (from N₂ emission fitting used to characterize plasma). It can be seen by the spectra in figure 12 that as the vibrational temperature increases, the prominent v=0 peak decreases and the smaller v=1 peak increases. At high enough vibrational temperatures such as 2400 K, the v=2 peak also starts to become noticeable as displayed in figure 12. This trend agrees with theory since at higher vibrational temperatures, the populations of vibrational levels above the ground state are more occupied due to an increase in energy in the molecular system. For all of the CARS spectra obtained (flame or plasma) the experimental data was fit against the best-fit theoretical spectrum and the vibrational temperature was found. To find the most accurate vibrational temperature, the deviation between experimental and theoretical spectra was quantitatively found by summing the absolute difference between spectral points and obtaining a χ^2 value defined by equation 6.

$$\chi^2 = \sum | \text{difference in spectral points} |^2 \quad (6)$$

After obtaining a series of theoretical spectra at different vibrational temperatures via CARSFIT, a chi-square distribution was plotted by MATLAB for each experimental spectrum against the various vibrational temperatures. MATLAB was programmed to automatically normalize the theoretical spectra to the experimental spectrum to ensure proper scaling. At the lowest point on the y-scale (or smallest χ^2) of the chi-square plot, the theoretical spectrum was the closest fit to the experimental spectrum; therefore, the vibrational temperature was found. After all of the averaged vibrational temperatures were found, the chemical kinetics modeling program Kintecus¹³ was used to simulate a

kinetic model with the conditions present in the experiment. The simulation took into account all of the energy-transfer processes in the flow between all of the species present in their correct concentrations. The primary processes that contributed to the kinetic model were vibrational-translational (V-T) and vibrational-vibrational (V-V) energy transfer from molecular collisions between species in the flow. By using given rates for all of the relevant energy-transfer reactions (molecular collisions) and parameters known during the experiment (pressure, temperature, probe time, etc.), the program was able to simulate the vibrational relaxation that occurred.

CHAPTER III

RESULTS

Pre-NTE measurements

Before running the CARS experiment in the NTE facility the RF-plasma had to be characterized by observing the emission of N_2 after contact with the plasma. Also, the experimental method had to be validated by successfully obtaining CARS spectra at room temperature and atmospheric pressure. After testing the setup variations and beam configurations at room temperature, the experiment was run in a flame to stimulate the population of the $v=1$ vibrational state and produce a $v=1$ peak in the CARS spectrum.

Plasma characterization by N_2 emission

An emission spectrum of N_2 was taken at a pressure of 25 Torr in the NTE tunnel with a plasma power of 140 W. Simulated spectra were compared to the experimental spectrum obtained, and the best-fit theoretical spectrum yielded a vibrational temperature of 2935 K \pm 18 K and a rotational temperature of 340 K \pm 4 K. The experimental emission spectrum and best-fit simulated spectrum of N_2 are shown in figure 13.

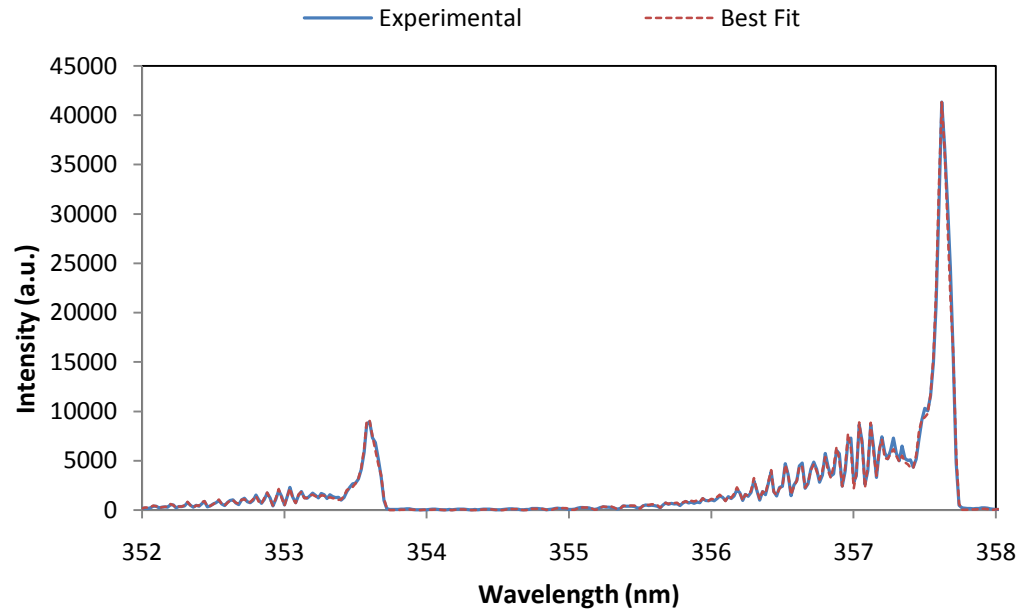


Figure 13. N₂ experimental emission spectrum and best-fit emission spectrum

The spectra shown in figure 13 are almost indistinguishable verifying that the fitting for the emission data was precise. The T_v and T_r values were obtained and the plasma-characterization diagnostics were run successfully. The rotational temperature found from the emission fitting is constant throughout the flow because the excess rotational energy is dissipated immediately after excitation; therefore 340 K was the rotational temperature exhibited in all CARS measurements.

CARS data from ambient air and flame

Before collecting data from the NTE tunnel, the setup and beam configuration had to be optimized to produce the maximum CARS signal at atmospheric pressure. The pressures in the NTE tunnel reach around 20 Torr and the CARS signal intensity is proportional to

the square of the gas density; therefore, the signal intensity will decrease exponentially in the NTE tunnel relative to the atmospheric conditions.¹⁴ The first set of spectra obtained were from N₂ CARS via the collinear beam configuration. At 1 atm pressure and standard temperature, the $v=0$ peak was found to have the largest intensity obtainable with some measurements reaching the saturation point (~ 60000 on intensity scale) at low integration times. One N₂ collinear-CARS spectrum at standard temperature and pressure in air (78% N₂) is shown in figure 14.

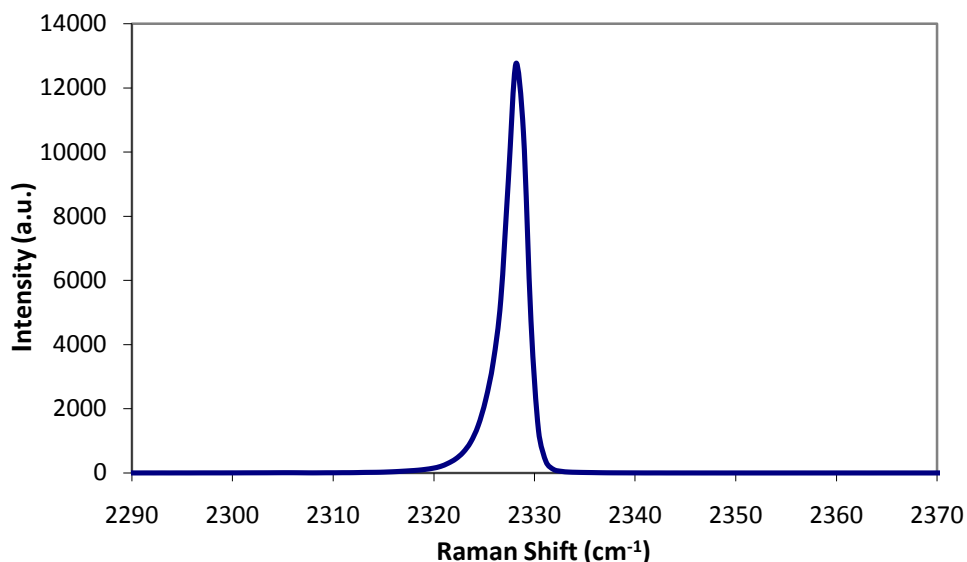


Figure 14. Collinear-CARS spectrum of N₂ at 1 atm and 298 K

The collinear beam arrangement gave good results for standard conditions, but when the flame was introduced at the interaction point the result was problematic in comparison with theory. The expected observation was the presence of the $v=1$ peak in the spectrum showing that the energy transmitted from the flame was populating the $v=1$ state in N₂.

This observation serves as a standard since the effect should be the same when molecules pass through the plasma in the NTE tunnel. However, the collinear interaction did not provide an accurate $v=1$ population as can be seen from the spectrum in figure 15.

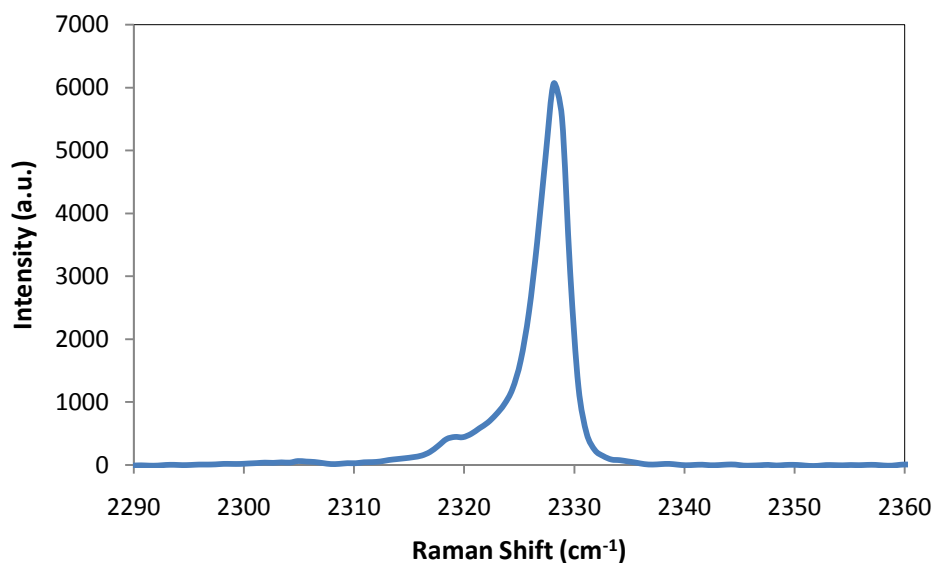


Figure 15. Collinear-CARS spectrum of N_2 in propane flame

As can be seen from figure 15, no distinguishable $v=1$ peak is present in the collinear-flame spectrum, only slight broadening. Similar to figure 14, the $v=0$ peak is displayed in the spectrum with relatively high intensity but the location of the $v=1$ peak is almost absent of signal other than a broadening of the larger peak. The failure of the collinear variant to accurately display the excited vibrational state is due to the over-representation of the ground state N_2 . The interaction region defined by equation 5 is large in comparison to the area of the flame where the measurements were made. The

large distance of interaction leads to the probing of N_2 molecules outside of the flame which were undisturbed by the flame. An accurate spectrum should provide measurable evidence of the $v=1$ population as well as a decrease in the $v=0$ peak compared to the intensity in figure 15. To alleviate the problems associated with the collinear setup, the boxCARS variant was setup and N_2 was observed in ambient air and in the propane/air flame. One of the first spectra taken via boxCARS (single species) in ambient air (78% N_2) is shown in figure 16.

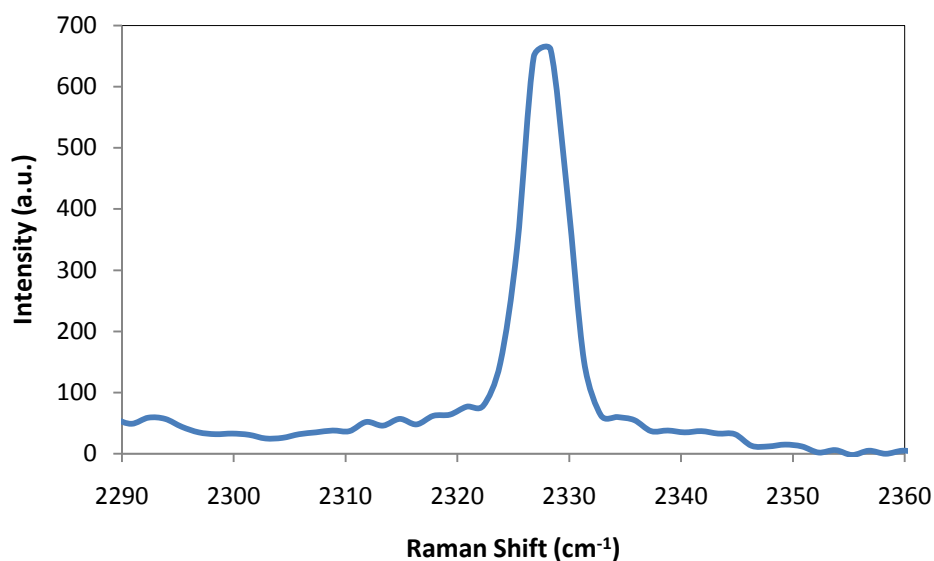


Figure 16. BoxCARS spectrum of N_2 in ambient air

The N_2 boxCARS spectrum at standard conditions was identical to the collinear spectrum except for a decrease in intensity. However, the flame spectrum yielded from the boxCARS variant gave results that agree with theory and therefore can be proven to give accurate and measurable results. The resultant boxCARS-flame spectrum of N_2

taken with an integration time of 10 s with its best fit theoretical spectrum is shown in figure 17(a) and the corresponding chi-square plot is shown in figure 17(b).

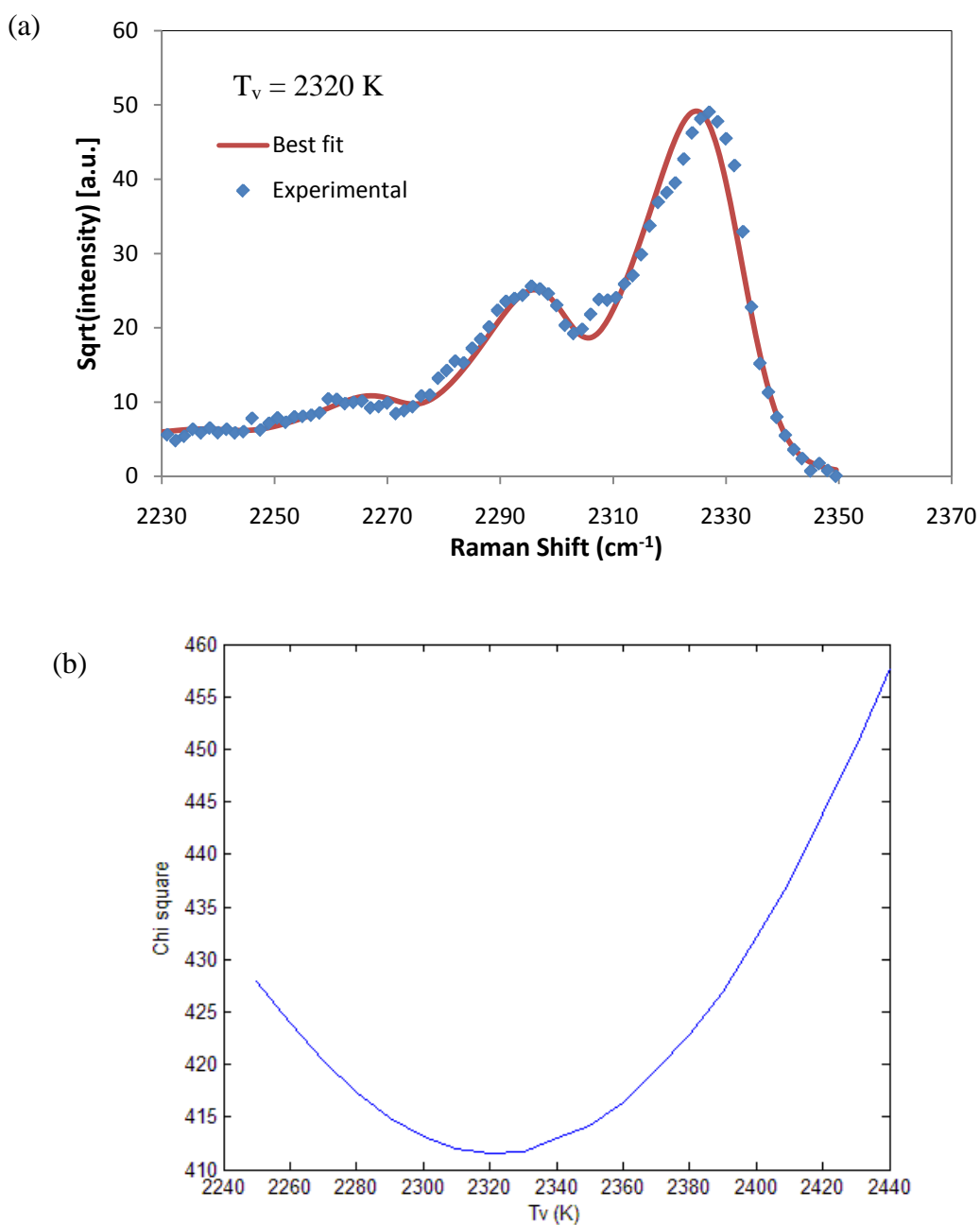


Figure 17. (a) Experimental CARS spectrum of N_2 in propane/air flame with theoretical fit. (b) Chi-square plot of N_2 flame spectrum compared with calculated spectra at various T_v

The flame spectrum taken by the boxCARS beam configuration was shown to have a distinct $v=1$ peak which was then fit to a theoretical spectrum calculated by CARSFIT. The theoretical spectrum in figure 17 was calculated with the following parameters: $P = 1$ atm, probe beam line-width = 10 (FWHM), pump beam line-width = 0.75 (FWHM), 0.80 N_2 mole fraction. The calculated T_v and T_r temperatures obtained from the CARSFIT theoretical spectrum shown in figure 17 was $T_v = 2320$ K and $T_r = 1600$ K. The result of the flame spectrum was in agreement with theory and it verified that CARSFIT calculations were precise. The flame spectrum in figure 17(a) was taken using the dual-pump CARS experimental setup. The O_2 peak disappeared immediately after lighting the flame because it is the oxidant used in the flame; therefore O_2 is decomposed into other reaction products produced in the flame and none can be measured. The dual-pump CARS spectrum taken in air at 1 atm is shown in figure 18; the beam positions were optimized to give maximum signal intensity.

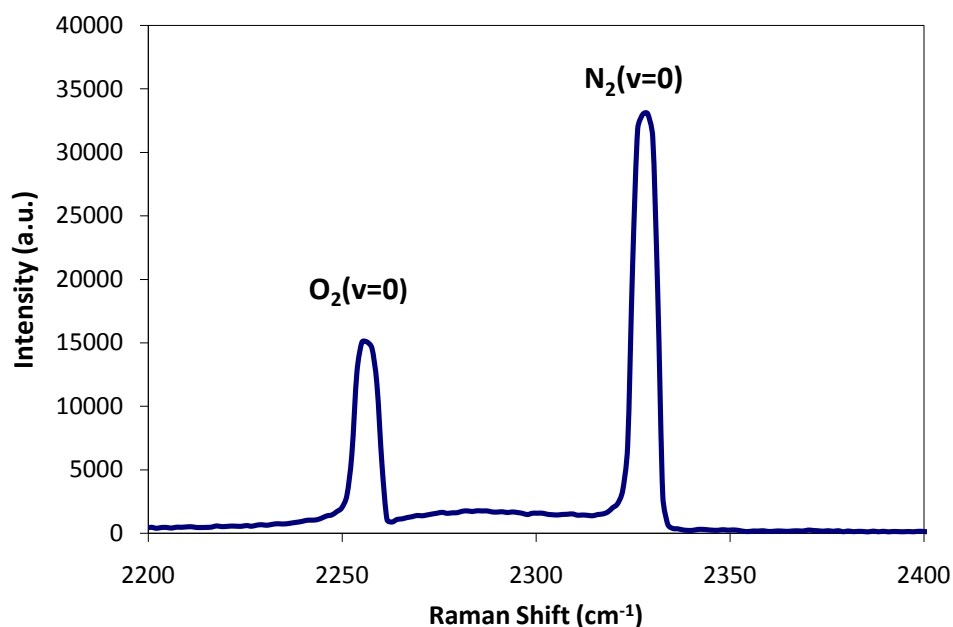


Figure 18. Dual-pump CARS spectrum of N₂ and O₂ at 1 atm and ~298 K

The larger peak in figure 18 is the N₂ (v=0) peak and the smaller is from O₂ (v=0). The spectrum was taken in standard conditions and integrated over 10 seconds. Figure 18 displays the ability of the dual-pump method to simultaneously probe N₂ and O₂ for vibrational measurements.

Measurement of vibrational relaxation in NTE-turbulent flow

Qualitative probing of vibrationally-excited N₂ and O₂ near plasma

To ensure that the plasma was successfully populating the v=1 state in O₂ and N₂, CARS spectra at position 1 (4.4 cm from plasma) were qualitatively analyzed before probing further down the flow since at position 1 the v=1 spectral peak should be the largest for

both species (more energy and $v=1$ population). The raw dual-pump CARS spectrum taken at 28 Torr pressure with an integration time of 10 seconds is shown in figure 19. The arrows in the plot indicate the expected Raman shifts (cm^{-1}) for each corresponding vibrational band in both N_2 and O_2 .

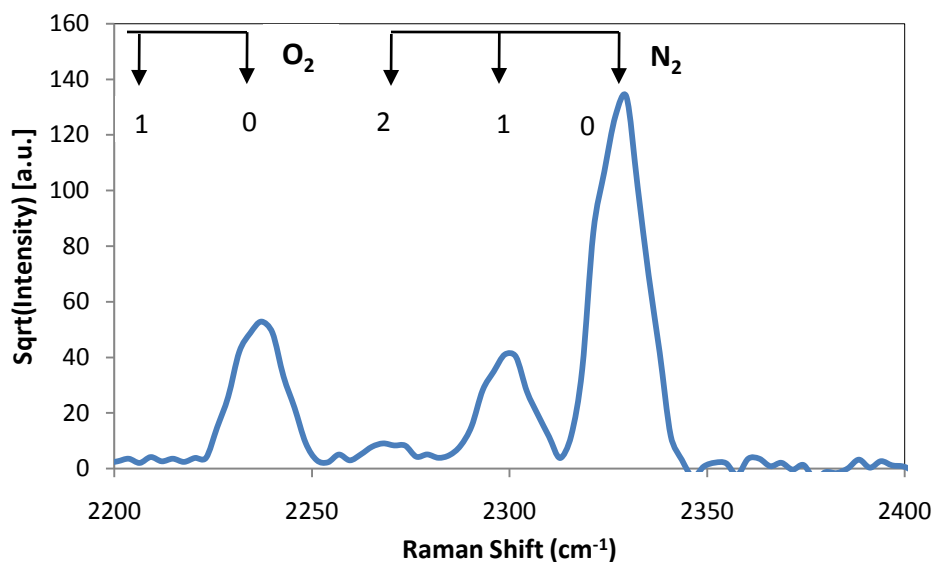


Figure 19. Dual-pump CARS spectrum 4.4 cm downstream

As seen from the spectrum in figure 19, the N_2 $v=1$ peak (2300 cm^{-1}) is relatively large displaying a reasonable population of N_2 in the $v=1$ state; the O_2 $v=1$ peak did not appear in the spectrum however, only the $v=0$ population was expressed. The lack of spectral representation of the O_2 $v=1$ vibrational state is likely due to two issues; 1) the high quenching rates of vibrationally-excited O_2 from collisions with background H_2O and 2) the low excitation probability given the mismatch between resonances in the electron scattering cross section of O_2 and the average electron energy of the plasma. Compared

with the relaxation time scale of N_2 , the lifetime of vibrationally-excited O_2 is considerably shorter. Due to the results shown in figure 19, only the vibrational temperatures found for N_2 could be quantitatively studied and modeled for vibrational relaxation kinetics.

Initial run with dual-pump boxCARS on N_2

The first measurements made in the NTE tunnel were done at a pressure of 28 Torr with a plasma power of 350 W. A total of five measurements were made along the flow axis at five different positions following the plasma. The first measurement was taken at 4.4 cm from the center of the plasma, the second was taken at 7.9 cm from the plasma, the third at 20.0 cm, the fourth at 26.5 cm, and the fifth at 39.4 cm; a schematic of the measurement positions through the test section is shown in figure 20(a) and a picture of the actual test section is displayed in figure 20(b).

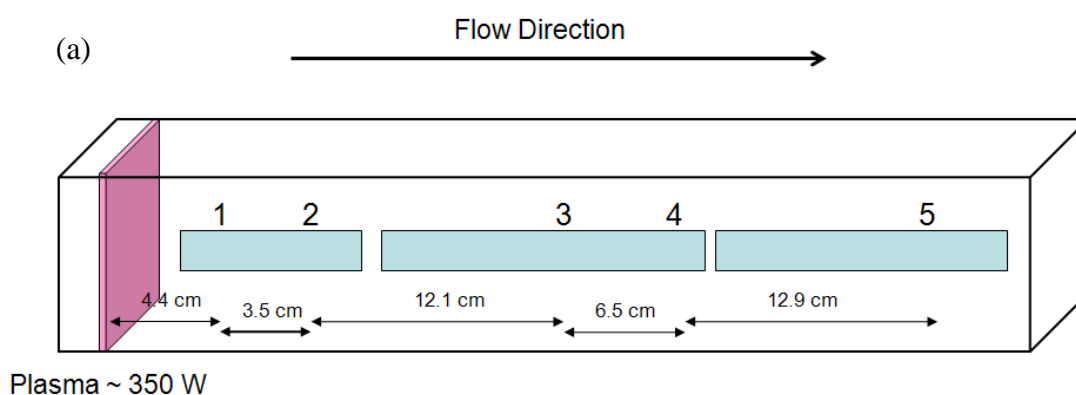


Figure 20. (a) Schematic of measurement positions

(b)

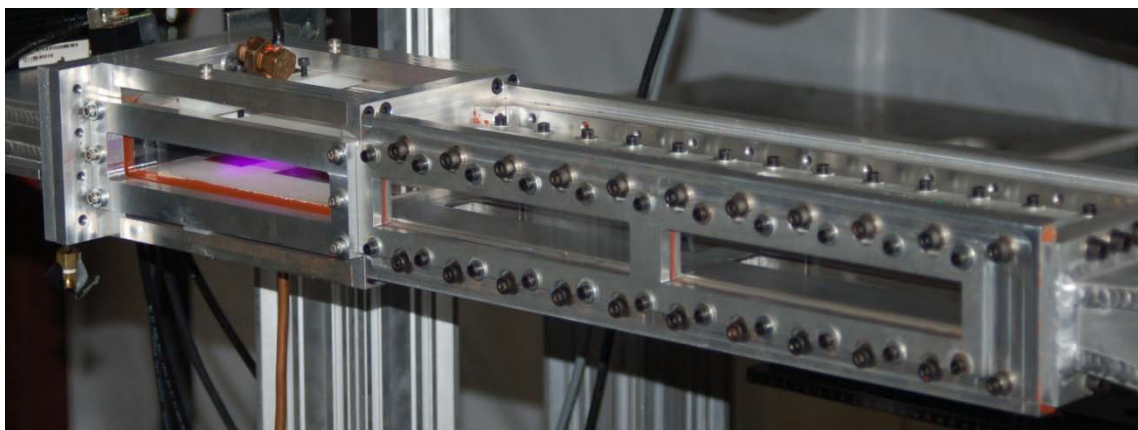


Figure 20. Continued. (b) Test section used in the experiment

According to the Boltzmann distribution found in equation 3, the decay of the $v=1$ population should be exponential as observed downfield from the plasma.

Approximately five spectra were taken at each position after background subtraction (for external interference elimination) and integration over 10 seconds. The overall intensity of the $v=1$ peak relative to the $v=0$ peak was not significantly large in comparison to the flame measurement; however, the $v=1$ state was populated enough to obtain measurements. A combination of chi-square calculations and CARSFIT fittings was used to obtain the T_v value for each run at each downfield position to a relative degree of accuracy. The theoretical spectra calculated by CARSFIT for NTE-tunnel data fittings were run under the following theoretical conditions: $P = 28$ Torr, probe beam line-width = 6-10 FWHM (different at different positions), pump beam line-width = 0.75 (FWHM), 0.80 N_2 mole fraction, $T_r = 340$ K. To obtain reasonable data of N_2 under NTE effects,

the RF-plasma was tuned to a power of 350 W and was adjusted so that it remained stable and uniform to ensure the thermal stability of the NTE system. The first spectrum taken at position 1 (4.4 cm downfield) is shown with the best-fit theoretical spectrum in figure 21(a) and the chi-square plot calculated by MATLAB is shown in figure 21(b).

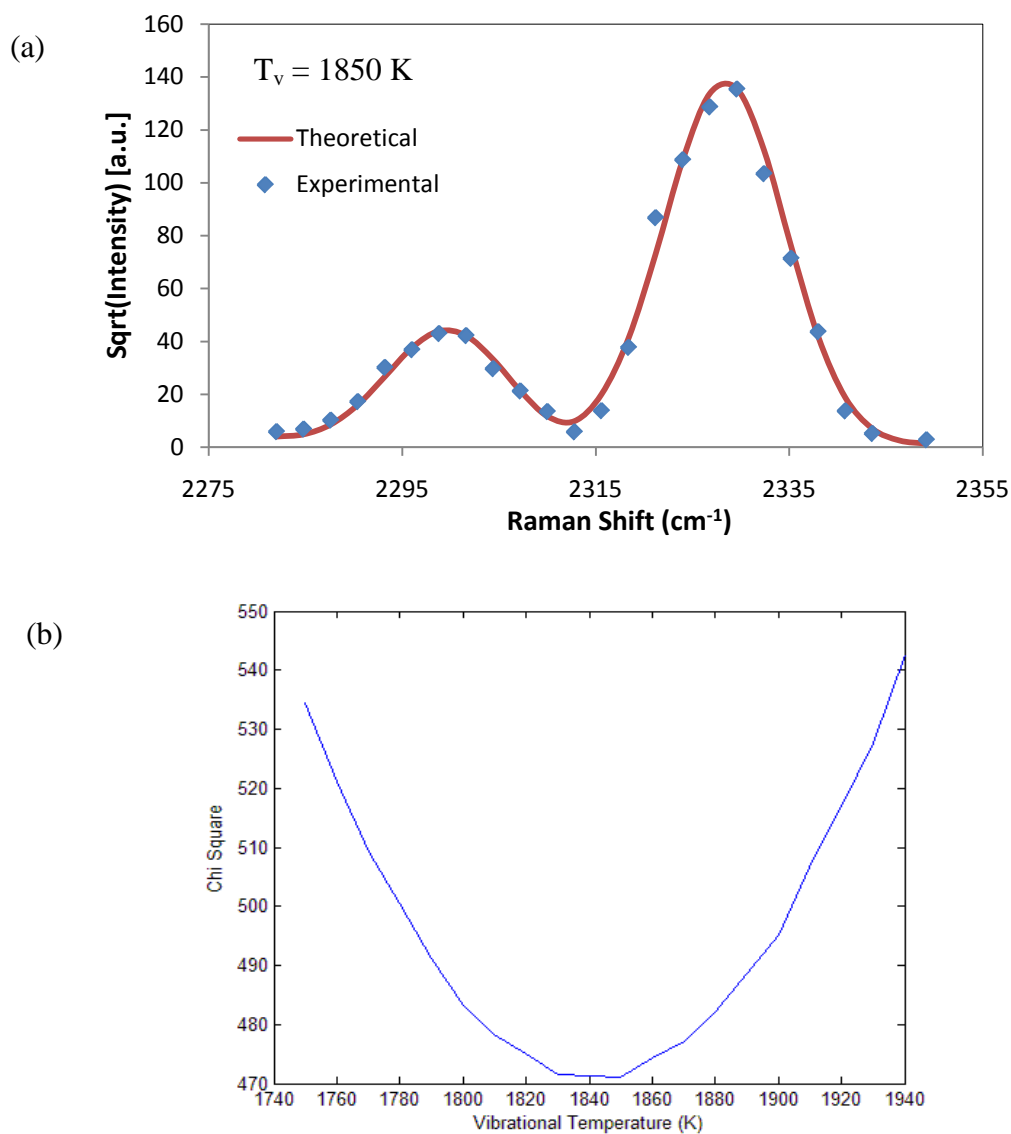


Figure 21. (a) N₂ CARS spectrum 4.4 cm downstream with best-fit theoretical spectrum. (b) Chi-square plot of N₂ spectrum compared with calculated spectra at various T_v

The T_v temperature obtained from the best-fit theoretical spectrum was 1850 K as seen from the minimum of the chi-square plot in figure 21(b). After analysis of all five spectra obtained at position 1 the average T_v value was found to be 1882 ± 46 K. The standard deviation between the five spectra was relatively small indicating that the chi-square analysis and experimental method were accurate in the spectra and subsequent T_v acquisition. The probe beam line-width for the measurements at position 1 was 10 FWHM; this was found by fitting simulated spectra at different line widths to the experimental spectra at position 1 to find the best fit. Position 2 was approximately 3.5 cm downfield from position 1 (7.9 cm from plasma) and five spectra were obtained. The first spectrum acquired at position 2 can be found in figure 22.

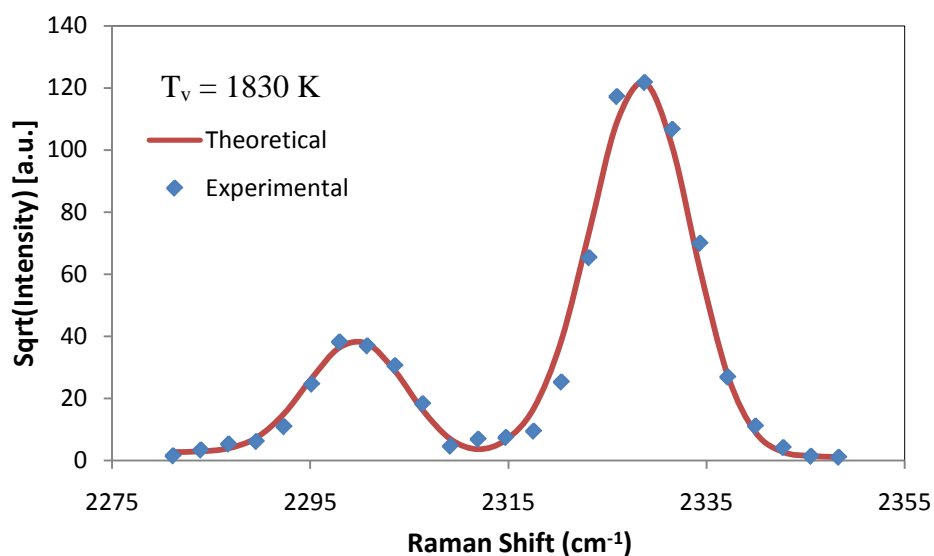


Figure 22. N_2 CARS spectrum 7.9 cm downstream with best-fit theoretical spectrum

The T_v temperature as found by the chi-square analysis in figure 22 was 1830 K. This result is close to what the approximate T_v should be given that position 2 is only 3.5 cm down the flow from position 1. The average vibrational temperature of N_2 at position 2 was found to be 1840 ± 50 K. The temperature dropped 42 K from position 1 resulting in a noticeable vibrational relaxation between position 1 and 2 thereby validating the data for kinetics measurements. The third measurement was taken at a position 20.0 cm from the plasma down the flow axis, and one of the five spectra that was obtained is shown in figure 23.

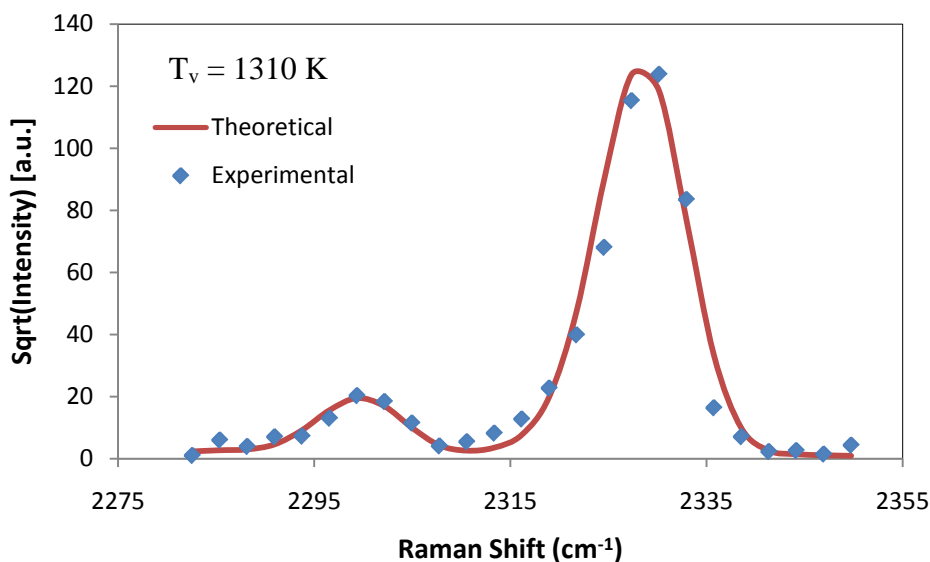


Figure 23. N_2 CARS spectrum 20.0 cm downstream with best-fit theoretical spectrum

As seen in figure 23, the relative $v=1$ peak height decreased dramatically from position 2 which was expected since the downfield distance was more than twice that of position 2. Significant vibrational relaxation occurred between positions 2 and 3. The line width of

the probe beam at position 3 was 7 FWHM and the CARSFIT theoretical spectra reflected that resolution. After analysis of all five spectra obtained at position 3, the average vibrational temperature was found to be 1324 ± 15 K. Given the low deviation of T_v values exhibited at position 3, the accuracy of the measurements and analysis proved fair. The fourth position that CARS measurements were made was 26.5 cm from the plasma down the flow, and the result of a single measurement with its best-fit theoretical spectrum is shown in figure 24.

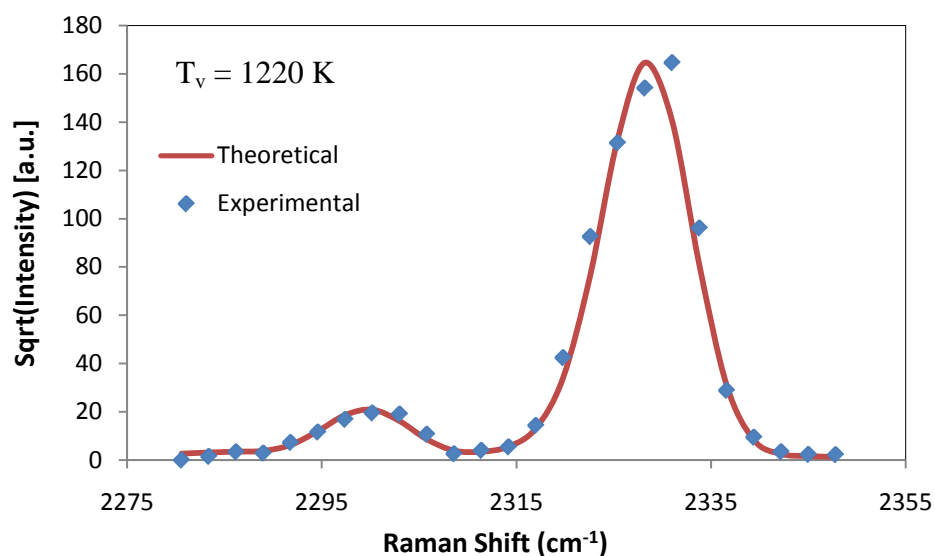


Figure 24. N₂ CARS spectrum 26.5 cm downstream with best-fit theoretical spectrum

Given that position 4 was approximately 6.5 cm further down the flow from position 3, a vibrational temperature decay of more than 100 K was observed. The final T_v value for position 4 after chi-square analysis of all five spectra was 1218 ± 33 K. The probe beam line-width did not change from position 3 so the CARSFIT parameters were kept

equivalent to those used for the position 3 calculations. The final CARS measurements that were taken in the subsonic-turbulent flow were at a distance of 39.4 cm from the induction of NTE. At the final position, the vibrationally-excited N_2 was expected to yield a vibrational temperature that was closer to vibrational equilibrium than the other four sets of measurements. One of the five spectra taken at position 5 is shown in figure 25.

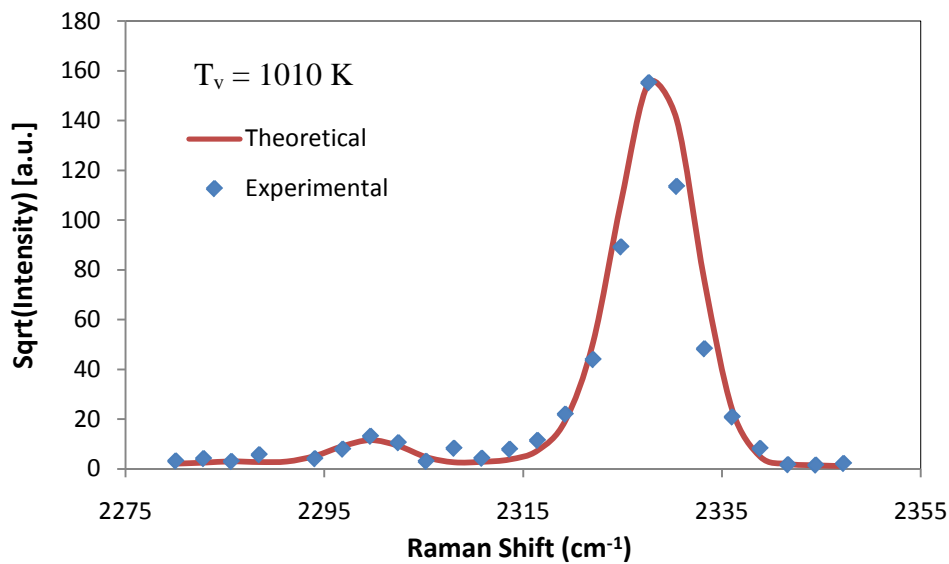


Figure 25. N_2 CARS spectrum 39.4 cm downstream with best-fit theoretical spectrum

As displayed in figure 25, much of the vibrationally-excited N_2 population has relaxed back down to ground state since the first measurement was made based on observing the relative $v=1$ peak intensities in the spectrum. The average vibrational temperature at position 5 was found to be 1010 ± 16 K. As expected, the vibrational temperature was lowest at the furthest position from the plasma since the N_2 had time to relax closer to equilibrium by transferring its vibrational energy via collisions with other incident

molecules in the flow. The probe beam line-width at position 5 was 6 FWHM and the theoretical fittings reflected that line width. The data collected from the CARS measurements and theoretical fittings yielded the vibrational relaxation of N_2 under NTE conditions as a function of distance and time following NTE-induction (plasma). The vibrational relaxation is shown as the decrease in T_v with distance and time in figure 26; the simulated fit calculated by Kintecus¹³ is shown as the curve in figure 26.

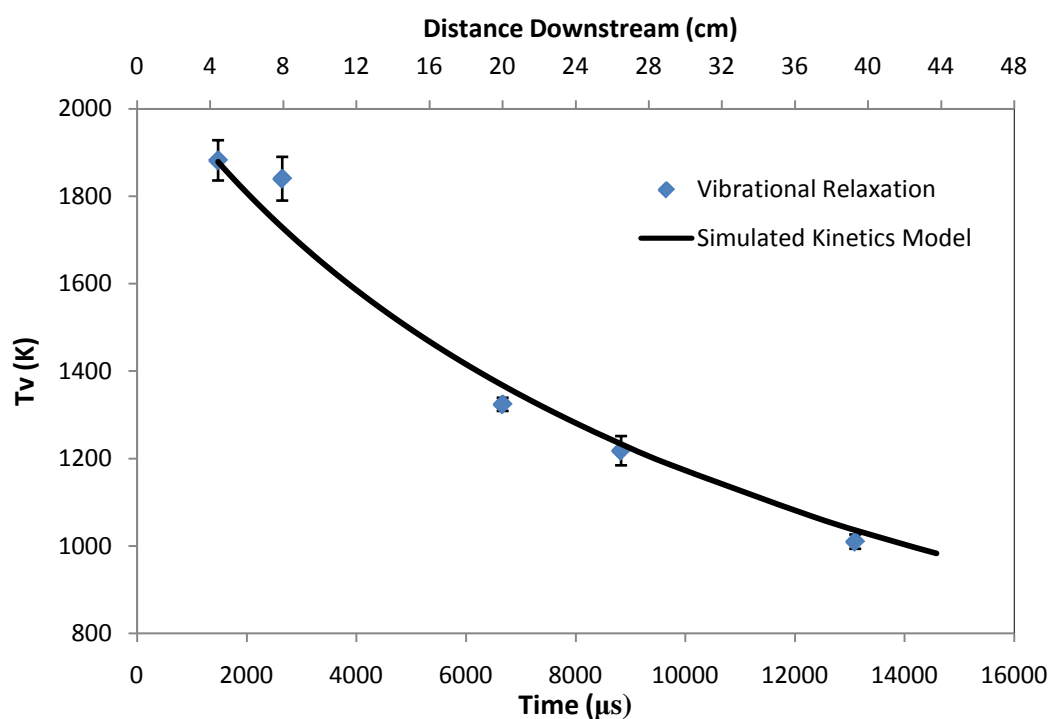


Figure 26. N_2 T_v decay under NTE-turbulence with time (μs) and distance downstream (cm)

Comparing the vibrational temperatures observed in the experiment with the Kintecus fit, the vibrational relaxation was accurate and consistent with the kinetics model. By confirming the accuracy of the vibrational relaxation observed via CARS, the energy-

transfer processes and molecular collisions in the system occurred at rates that were expected for the flow under study. The Kintecus model was calculated using conditions equivalent to those present during the experiment. A plot similar to figure 26 displaying the vibrational relaxation of N_2 in terms of the decay of the $v=1$ spectral intensity, $I_{v=1}$, normalized to the intensity of $v=0$, $I_{v=0}$, is shown in figure 27.

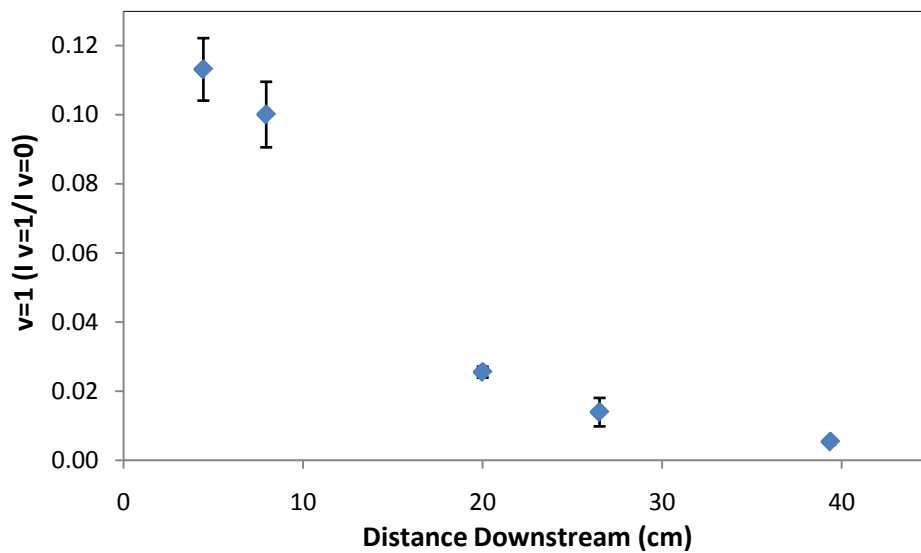


Figure 27. % $v=1$ spectral-intensity decay with distance along flow axis

Displayed in figures 26 and 27 is a small decay followed by a rapid loss of vibrational energy after approximately 8 cm. The N_2 molecules seem to retain much of the energy gained from plasma-excitation until a release after a certain time or distance past the initial excitation. Part of the reason for the rapid decay may be quenching effects due to the shape of the turbulent flow. At approximately 26.5 cm down the flowfield from the plasma, the rapid decay seems to bottom-out and return to somewhat gradual relaxation.

A table of the T_v values and $I_{v=1}/I_{v=0}$ ratios observed from the CARS measurements in the NTE tunnel is shown in table 1.

Table 1. T_v and $I_{v=1}/I_{v=0}$ data observed at distances down the flow-axis, z , when $z_0 =$ distance at plasma

<i>Distance Past Plasma (cm)</i>	$z_1 = 4.4$	$z_2 = 7.9$	$z_3 = 20.0$	$z_4 = 26.5$	$z_5 = 39.4$
T_v (K)	1882 ± 46.0	1840 ± 50.0	1324 ± 15.0	1218 ± 33.5	1010 ± 16.3
$I_{v=1}/I_{v=0}$	0.113 ± 0.009	0.100 ± 0.009	0.025 ± 0.001	0.014 ± 0.004	0.005 ± 0.000

The results of the first attempt to model N_2 vibrational relaxation via CARS spectroscopy were used successfully, and initial results are in agreement with the hypothesis made. More iterations of the experiment are to be made to eliminate experimental uncertainty by acquiring more data sets. However, comparing the experimental vibrational relaxation with the simulated relaxation indicates that the vibrational temperatures were accurate. Dual-pump CARS was successful in accurately measuring the vibrational temperatures of N_2 after vibrational excitation; ground state O_2 was detected with ease, but no vibrationally-excited O_2 could be detected because of the rapid quenching rates of O_2 at the RF-plasma conditions available in the experiment.

CHAPTER IV

SUMMARY AND CONCLUSIONS

The vibrational NTE and relaxation of N_2 was successfully probed in a subsonic flowfield via CARS spectroscopy. First, collinear CARS and boxCARS beam variants were both tested through ambient air and flames to determine the optimal setup that would yield accurate results. It was found that the collinear laser-beam configuration probed a large interaction length consequently disrupting the accuracy of the results by over-representing the ground state ($v=0$) molecules in the CARS spectrum. BoxCARS proved to accurately represent the populations of the vibrational states by decreasing the interaction region by more than a factor of 10 thereby giving better spatial resolution. The success of probing N_2 through a propane/air flame by boxCARS was evidence that boxCARS was the CARS variant that would yield measurable results from the NTE tunnel. N_2 emission data showed that the RF-plasma would serve as a proper NTE-induction mechanism and that energy would be transferred to N_2 and O_2 vibrational modes with minimal gas heating; this was verified by the fitting of the emission spectrum that yielded a rotational temperature of 340 ± 4 K. CARS measurements of N_2 were taken at various locations in the subsonic NTE tunnel at a flow velocity of approximately 30 m/s. The experiment was run at subsonic flow speeds as a precursor to supersonic and hypersonic NTE measurements. By successfully modeling the time-resolved vibrational relaxation through the NTE-turbulent flow at subsonic speed, the data gives insight into NTE-turbulence coupling and the expected model that future

hypersonic measurements will yield. The signal/noise ratio of the initial measurements through the cold-flow NTE were good and a definite vibrational relaxation of N_2 was observed. Spectral data yielded the vibrational temperatures (T_v) of N_2 at positions downstream the plasma. The T_v values of N_2 at distances of 4.4 cm, 7.9 cm, 20.0 cm, 26.5 cm, and 39.4 cm down the flow from the plasma were 1882 ± 46 K, 1840 ± 50 K, 1324 ± 15 K, 1218 ± 33 K, and 1010 ± 16 K respectively. The decay of the vibrational temperature and the normalized $v=1$ ($I_{v=1}/I_{v=0}$) decay were both modeled as functions of distance and time past the cold-flow NTE induction.

The results of the vibrational relaxation were in agreement with theory and proved that CARS was a successful technique to model the relaxation of air whether through subsonic or hypersonic flows. Dual-pump CARS was successful in probing N_2 and O_2 simultaneously, but vibrationally-excited O_2 could not be measured due to the rapid quenching of vibrational energy at electron energies available to the RF-plasma. More experimental iterations are needed to collect a complete data set of CARS measurements to ensure the absolute accuracy of the results from N_2 measurements. The pathways for energy transfer from vibrationally-excited N_2 and O_2 will be examined with all of the combined data, and the rates of energy-transfer processes such as quenching, vibrational-translational, vibrational-vibrational, and vibrational-rotational energy transfer will allow a complete kinetic model to be built based on all of the data collected.

Further research will complete the overall kinetic model of vibrational relaxation of air molecules in turbulent flows; however primary experiments validated CARS spectroscopy as an apt technique to measure the vibrational temperatures of N_2 and O_2 and subsequently the vibrational relaxation of N_2 to understand the coupling of NTE and turbulence. The result of probing N_2 via CARS has yielded initial understanding of the quantum mechanics in NTE flow and the energy-transfer mechanisms that occur in NTE flows. The insight achieved by the experiment leads to applications in hypersonic flight where NTE governs the thermochemical processes present in turbulent flow over hypersonic objects. Also, the coupling between NTE and turbulence can be quantitatively expressed and applied to a model that allows accurate calculations of hypersonic processes to be used in aerospace and chemical research.

REFERENCES

1. Mitcheltree R, Gnoffo P. *Journal of Spacecraft Rockets* 1991; **28**: 552.
2. Mitcheltree R, Shebalin J. *Journal of Spacecraft and Rockets* 1992; **29**.
3. Hsu A, Srinivasan R, Bowersox R, North S. *Application of Molecular Tagging Towards Simultaneous Vibrational Temperature and Velocity Mapping in an Underexpanded Jet Flowfield: AIAA Journal* (to be reviewed).
4. Harvey, AB. *Chemical Applications of Nonlinear Raman Spectroscopy*. Academic Press, Inc.: New York, 1981.
5. Smith M, Coblish J. *24th AIAA Aerodynamic Measurement and Ground Testing Conference*. 2004.
6. Alden M, Edner H, Svanberg S. *Phys. Scr.* 1983; **27**: 29.
7. Greenhalgh DA. *J. Raman Spectrosc.* 1983; **14**: 150.
8. Dudovich N, Oron D, Silberberg Y. *Nature* 2002; **418**: 512.
9. Malarski A, Beyrau F, Leipertz A. *J. Raman Spectrosc.* 2005; **36**: 102.
10. Beyrau F, Seeger T, Malarski A, Leipertz A. *J. Raman Spectrosc.* 2003; **34**: 946.
11. Lucht R. *Opt. Lett.* 1987; **12**: 2.
12. Farrow R, Lucht R, Clark G, Palmer R. *Appl. Opt.* 1985; **24**: 2241.
13. Ianni, JC. Kintecus v3.95, Windows Version. <http://www.kintecus.com>, 2008.
14. Eckbreth, AC. *Laser Diagnostics for Combustion Temperature and Species*, 2nd edn. Gordon and Breach: Amsterdam, 1996.

CONTACT INFORMATION

Name: Jacob Dean

Professional Address: c/o Dr. Simon North
Department of Chemistry
Texas A&M University
College Station, TX 77843

Email Address: deanugus@yahoo.com

Education: B.S., Chemistry, Texas A&M University, May 2009
Cum Laude
Undergraduate Research Scholar